communications materials

Review article

https://doi.org/10.1038/s43246-024-00468-6

Interstitial fluid-based wearable biosensors for minimally invasive healthcare and biomedical applications

Check for updates

Zixiong Wu [1,6], Zheng Qiao[1,6], Shuwen Chen[2,7] ✉, Shicheng Fan[1], Yuanchao Liu[3], Jiaming Qi[1] & Chwee Teck Lim [1,4,5,7] ✉

Interstitial fluid (ISF), a biological fluid rich in diverse biomarkers and analytes and similar to blood composition, has garnered significant attention as a valuable source of clinically relevant information. Consequently, ISF-based wearable biosensors are emerging as powerful tools for non-invasive and minimally invasive disease diagnosis, personalized medicine, and other healthcare and biomedical applications. This review provides a comprehensive overview of recent advancements in ISF-based biosensors, with a particular focus on wearable ISF sensors. We first offer insights into ISF biomarkers and sampling techniques and discuss recent ISF sensing strategies that encompass materials, fabrication methods, and sensing mechanisms. Then, we present a comprehensive overview of their applications. Finally, we address the challenges faced in this field and offer a forward-looking perspective on promising future directions.

Interstitial fluid (ISF), which exists in extracellular spaces and directly diffuses from blood vessels holds great potential for healthcare and biomedical applications. It is one of the epidermally accessible biofluids and has a similar composition to blood[1]. Various target biomarkers are present in ISF and can be detected by ISF-based wearable biosensors to provide vital information critical to both clinicians and patients[2–4]. Thus, ISF and ISF sensors can offer insights into disease diagnosis, progression, and even holistic health conditions.

While blood or blood serum remains the primary biofluid and has often been considered the gold standard for detecting numerous biomarkers, its collection involves invasive hypodermic needles, necessitating professional expertise for safe retrieval[5,6]. This approach restricts frequent blood sampling and biochemical assessments outside clinical settings, except for specific techniques such as finger-pricking for blood glucose monitoring. Over the years, researchers have earnestly pursued alternative methods that maintain accuracy while reducing invasiveness and complexity.

These explorations center on identifying a biofluid that is similar to blood, easily accessible with minimal invasiveness, to serve as a transformative game-changer in diagnostic procedures. These easily accessible biofluids which include ISF[3,5,7], tears[8,9], saliva[10,11], and sweat[12,13] were proposed and studied to evaluate both small (e.g. glucose, lactate, and amino acids[14]) and large molecules (e.g. drugs[15], proteins[16], and hormones[17]) biomarkers. Among these biofluids, ISF shows advantages both in large amounts, low bio-interference, and high clinical relevance. To fully utilize ISF sensors for facilitating healthcare applications, extensive research has been conducted to withdraw information from ISF reliably, simply, and minimally invasively. It not only involves sampling or accessing ISF through microneedles[18–20], reverse iontophoresis (RI)[21–23], and micro-dialysis[24], but also includes measuring ISF biomarkers[25,26] such as metabolic species and drugs to provide diagnosis and management of diseases.

In this review, we report recent progress made in ISF sensors for healthcare applications (Fig. 1). We first introduce the ISF bioenvironment, biomarker compositions, and sampling techniques. Second, we summarize the ISF sensing technologies for small molecules or macromolecule monitoring. We then discussed ISF-based biochemical sensors for healthcare applications such as disease diagnosis and drug assessment. While outlining recent advancements in this field, we will also delve into some of the challenges and suggest forthcoming innovations and directions for the future.

[1]Department of Biomedical Engineering, National University of Singapore, Singapore, Singapore. [2]Institute of Medical Equipment Science and Engineering, Huazhong University of Science and Technology, Wuhan, China. [3]Department of Physics, City University of Hong Kong, Hong Kong SAR, China. [4]Institute for Health Innovation and Technology (iHealthtech), National University of Singapore, Singapore, Singapore. [5]Mechanobiology Institute, National University of Singapore, Singapore, Singapore. [6]These authors contributed equally: Zixiong Wu, Zheng Qiao.[7]These authors jointly supervised this work: Shuwen Chen, Chwee Teck Lim. ✉e-mail: shuwenchen@hust.edu.cn; ctlim@nus.edu.sg

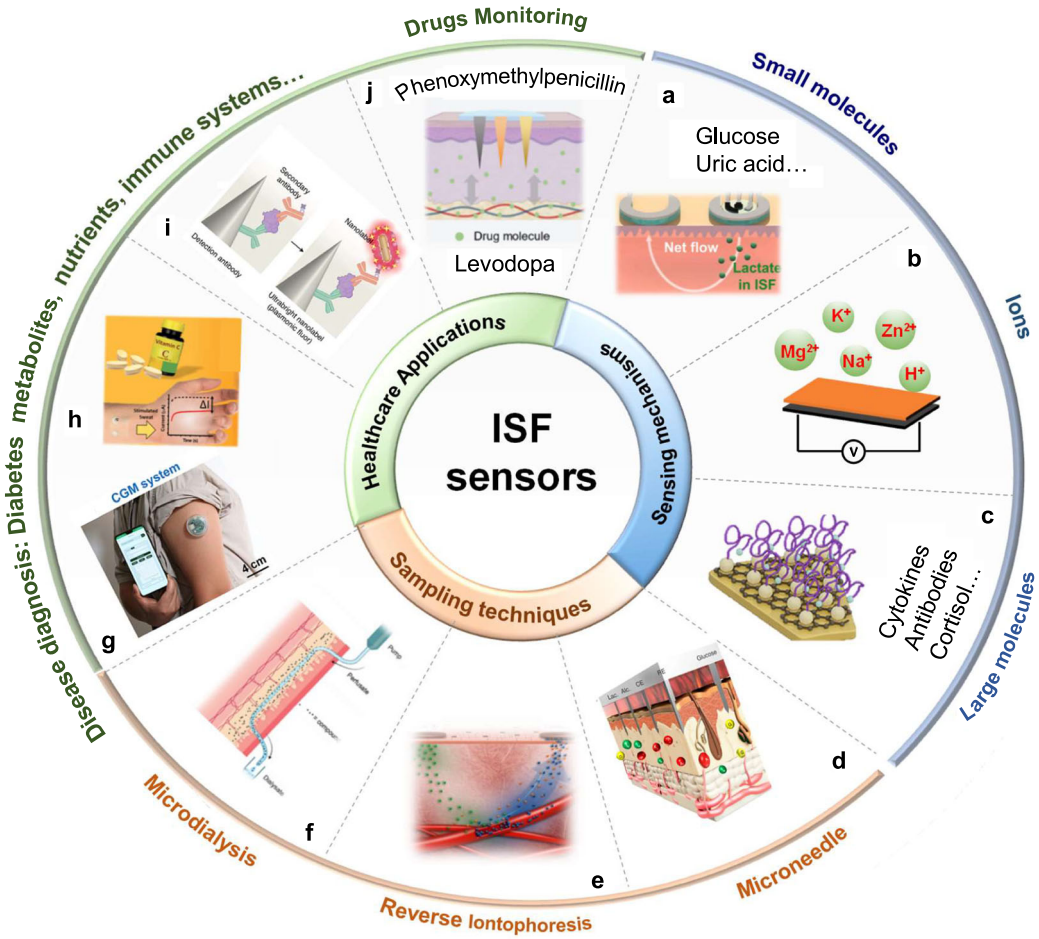

Fig. 1 | Overview of ISF-based wearable biosensors for healthcare. a Small molecule sensing mechanisms, reproduced with permission from ref. [104], copyright 2023, American Chemical Society. **b** Ions sensing mechanisms. **c** Large molecule sensing mechanisms[90]. Reproduced under the CC BY-NC 4.0 license. **d** Microneedle-based sampling methods to access ISF. Reproduced with permission from ref. [25], copyright 2022, Springer Nature Limited. **e** Reverse Iontophoresis-based sampling methods to withdraw ISF. Reproduced with permission from ref. [140], copyright 2020, MDPI. **f** Microdialysis mechanism[141]. Reproduced under the CC BY-NC 4.0 license. **g** Continuous glucose monitoring by accessing ISF for diabetes management. Reproduced with permission from ref. [45], copyright 2023, American Chemical Society. **h** Nutrient monitoring using ISF. Reproduced with permission from ref. [105], copyright 2023, American Chemical Society. **i** Cytokine and protein measurements. Reproduced with permission from ref. [121], copyright 2021, Springer Nature Limited. **j** Drug monitoring using microneedle-based technologies[15]. Reproduced under the CC BY-NC 4.0 license.

ISF biomarkers

Skin is the largest organ of the human body, comprising three primary layers, epidermis, dermis, and hypodermis[27] (Fig. 2a). The dermis contains the largest amount of ISF. Due to its rich capillary network facilitating real-time nutrient exchange with ISF, the dermis is regarded as the ideal location for extracting ISF. ISF is the predominant extracellular fluid within the human body, surpassing blood plasma in volume by nearly three times[28]. It plays a vital role in nutrient transport, waste removal, and signal transport with blood. The ISF is endowed with biomarkers that exhibit an analogous compositional profile to that of blood plasma, thereby making it suitable as a target for biomarker detection, and yet is free from pain and clot formation as seen in traditional blood sampling techniques. However, despite the relatively easy access to ISF, the concentration of some of its biomarkers may deviate from that of the blood plasma, due to the blood having to pass through both size and charge barriers before entering the ISF compartment. During biomarker translocation from blood plasma to ISF, species endowed with charge or large molecular dimensions, such as proteins, will encounter impediments that may prevent them from passing through the intervening barriers. Consequently, this phenomenon results in the difference in biomarker concentrations between ISF and blood plasma. The regulation of biomarker permeability, particularly concerning variations in size, predominantly relies on the integrity and function of inter-endothelial junctions (IEJs), which encompass cadherin junctions and tight junctions[29].

The relationships between biomarker concentrations in ISF and blood plasma are depicted in Table 1 and Fig. 2d. Small molecules with a molecular weight below 3 kDa, such as ions, glucose, and urea, can passively diffuse across the cellular capillary wall[1]. Consequently, these biomarkers exhibit almost similar concentrations in the ISF as that in the blood plasma. In the context of biomarkers falling within the size range of larger than 3 kDa and yet less than 70 kDa like insulin, cytokines, and albumins, it is discernible that size-related impediments partially constrict their transportation. In this scenario, a collaborative interplay between paracellular and transcellular transportation mechanisms regulates the transit of these biomarkers. Taking albumins as an example, studies show that the concentration of albumins in the ISF is observed to be reduced by approximately 52% in comparison to their counterparts in the blood plasma in the human leg[30]. In the case of biomarkers with a molecular weight exceeding 70 kDa, their concentration in the ISF is significantly reduced. This is due to passive diffusion ceasing to be an effective means of transportation for biomarkers of such size, and transcytosis dominates the transportation of these biomarkers[31]. However, this balance can be disrupted in the presence of inflammation in the superficial subcutaneous tissue[32]. The subsequent

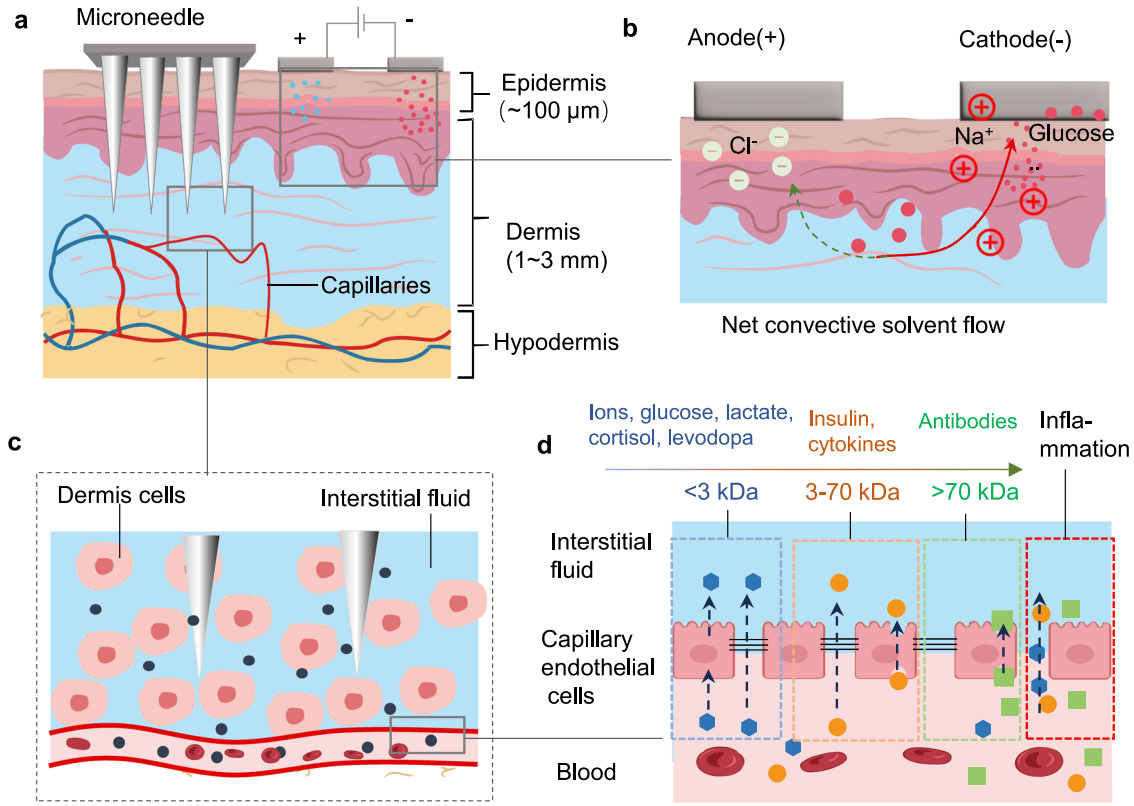

Fig. 2 | ISF biomarker, size, and bioenvironment. a Schematic illustration of skin structure, ISF bioenvironment, and common ISF accessing approaches. **b** Schematic illustration of reverse iontophoresis-based ISF sampling approach and bioenvironment. **c** Schematic illustration of microneedle accessing or sampling approach and bioenvironment. **d** Transport pathways of biomarkers between blood and ISF.

immune response may impair the size selection of biomarkers, resulting in a disorderly concentration of biomarkers in the ISF.

The size of the target biomarkers also plays a crucial role in determining the appropriate methods for extracting ISF. For instance, certain techniques such as the suction blister method, micropores, and suction method may inflict tissue damage, thereby inducing inflammatory responses. This, in turn, has the potential to introduce distortions in the concentration of larger molecule biomarkers, such as proteins. A number of ISF sampling methods have been integrated with biosensors to realize minimally invasive healthcare applications, such as reverse iontophoresis[33,34] (Fig. 2b), microneedles[5,35–37] (Fig. 2c) and microdialysis[24]. Furthermore, it's worth noting that the reverse iontophoresis method and microdialysis and ultrafiltration methods have inherent limitations when it comes to detecting biomarkers, particularly those of larger size. These techniques can lead to a dilution of biomarker concentration, an effect that is particularly pronounced for biomarkers with substantial molecular dimensions[3,38].

Sampling techniques

The analysis of ISF holds significant clinical importance due to its minimally invasive nature, alleviating concerns related to clotting and interference from blood cells. While ISF harbors valuable biomarkers with significant clinical potential, it is challenging to sample or access for effective detection. To address this, numerous sampling methods have been proposed, including microneedles, reverse iontophoresis, and microdialysis. These techniques either extract ISF from the human body for external analysis or employ in-body sensors positioned within the tissue for in-situ real-time analysis.

Microneedle

Microneedle-based sampling methods utilize arrays of microneedles to breach the skin, establishing fluid pathways for the extraction of ISF. Microneedles can be classified into solid, hollow, porous, and hydrogel microneedles according to their materials and structures.

Solid microneedles. The solid microneedles are typically constructed in the shape of pyramids or cones, featuring a sharp tip. Solid microneedles are relatively simpler to fabricate, possess more robust mechanical properties, and are more cost-effective compared to other microneedle types[39]. Microneedles, when pressed onto and then removed from the skin, can create microchannels for ISF sampling or extraction. The ISF can be directly transported to these microchannels through osmotically driven flow, utilizing a concentration gradient to propel ISF into the channels. Sensors placed near these channels can then directly analyze the ISF components[20]. Additionally, negative pressure-driven convection, which creates a pressure differential between the dermal layer and the skin surface, can also be used to facilitate ISF movement to the microneedle-created microchannels for subsequent analysis[5]. Meanwhile, RI was also reported to promote the movement of ISF to the micropores for subsequent analysis[34]. Moreover, solid microneedles tailored with functional materials can be indwelled in dermis layer for in situ biomarker detection[25]. In this case, microneedle tips are directly metalized with electrode materials and subsequently functionalized with sensing elements to capture specific biomarkers and transduce signals for further processing. Owing to the capabilities to directly serve as sensors, they can be seamlessly integrated with other electronics and data collection systems for biomarker monitoring purposes. Corrie et al. were pioneers in introducing the concept of functionalized microneedle patches for specific biomarkers detection (Fig. 3a)[40]. This approach has been developed to detect clinically significant biomarkers such as glucose[41], drug[42], and even multiple biomarkers[25]. Although it can choose the target biomarkers by modifying microneedles, this method typically involves an additional step to elute captured biomarkers on microneedles for further in vitro analysis.

Table 1 | Summarization of ISF biomarkers and their relationship with blood

Targets		MW (Da)	Transport & access approaches	Recognition element	Sensing method	Concentration in ISF &blood	Health relations	Ref.
Electrolytes	Na^+	23	Paracellular diffusion Microneedles; Reverse iontophoresis; Microdialysis	Ionophores	Potentiometry, impedance spectroscopy, colorimetry, fluorescence	135–145 mM ≈ plasma	Cardiovascular disease, fluid balance, nerve function	2,3,5,108,109,133,134
	K^+	39		Valinomycin		3.5–5 mM ≈ plasma	Cardiovascular disease, fluid balance, nerve function, kidney function	2,3,108,109,133–135
Metabolites	Lactate	90		Lactate Oxidase	Amperometry,voltammetry, colorimetry, fluorescence	0.3–1.3 mM (resting) ≈ plasma	Lactic acidosis	2,3,122,136
	Glucose	180		Glucose Oxidase/ Dehydrogenase		3.9–7.1 mM ≈ plasma	Diabetes	2,3,34,41,45,55,96,137,138
Hormones	Cortisol	362		Aptamer/Antibodies	ELISA, colorimetry, fluorescence	140–690 nM (Total) 11–77 nM (unbound) ≈ unbound in plasma	Psychosocial stress, metabolic syndrome	2,3,115,116,139
Drugs	Levodopa	197		Carbon-based electrodes	Amperometry, voltammetry	Depends on drugs ≈ unbound in plasma	Parkinson's disease	3,44,122
	Phenoxymethylpenicillin	350		Enzymes			Antimicrobial resistance	122,124
Proteins	Cytokines	6-70k	Paracellular diffusion & transcellular diffusion Microneedles	Aptamer, Antibodies	ELISA, FLISA	pM-nM ≈ 80% in plasma	Cytokine storm	2,118,119,121
	Antibodies	150-970k	Transcellular diffusion Microneedles	Antibodies	ELISA, FLISA, Immunochromatography	0.4–16mg (total) ≈ 15–25% plasma	Infections	120,121

MW molecular weight, *ELISA* enzyme-linked immunosorbent assay, *FLISA* Fluorophore-linked immunosorbent assay.

Hollow microneedles. Hollow microneedles typically share the same morphological characteristics and fabrication materials as their solid counterpart. The hollow lumen of these microneedles serves a dual purpose, forming microchannels for ISF extraction and serving as a conduit for drug delivery. This method utilizes capillary flow to extract ISF from the dermis, inducing rapid convection within the lumen and establishing a concentration gradient that facilitates the extraction of ISF from the dermis for further analysis[7]. Ribet et al. put forward an integrated microneedle patch designed for ISF collection, characterized by its compatibility with clinical translation (Fig. 3b)[43]. This technology enables the concurrent monitoring of multiple analytes, spanning small molecules, antibodies, and proteins. The lumen can also be customized for direct biomarker detection within the dermis by inserting functional materials into the cavity. For instance, Gout et al. introduced a microneedle array in which the microneedles are coated with diverse carbon pastes, enabling both enzymatic and nonenzymatic monitoring of Levodopa (L-Dopa)[44]. A large number of studies have been focused on developing sensing technologies based on hollow microneedles[45–47]. A significant concern associated with the use of hollow microneedles is their susceptibility to blockage, primarily due to the cutting of dermal tissue during the insertion process[48].

Porous microneedles. Porous microneedles, characterized by numerous capillary channels, are typically constructed using polymer, metal, and inorganic materials[49]. These microneedles, when integrated with iontophoresis, can enable the extraction of ISF from the dermis to the sensing chamber for subsequent analysis[23]. For instance, Kusama et al. integrated iontophoresis with ion-conductive porous microneedles, further modifying them with charged hydrogels, resulting in a significant enhancement of extraction efficiency[50]. Apart from integrating with iontophoresis, porous microneedles can directly utilize capillary-driven channels to extract ISF for diagnosis. For example, Lee et al. proposed a system that seamlessly integrated porous microneedles with a glucose sensor, demonstrating commendable performance in both sample extraction and glucose measurement (Fig. 3c)[51]. Additionally, porous microneedle electrodes, owing to their microporous structure, exhibit a larger specific surface area, thereby providing more active sites for target detection[49,52].

Hydrogel microneedles. Hydrogel microneedles represent a novel category of microneedles that remain rigid in dry conditions and undergo swelling upon penetration into the dermis. The microneedle can be made of hydrogel or coated with it[53–55]. Hydrogel microneedles offer several distinct advantages when compared to their counterparts. Firstly, the stiffness of hydrogel microneedles can be readily adjusted by controlling the polymer crosslinking ratio, which is difficult for conventional microneedles[56]. Secondly, due to their swelling ability, hydrogel microneedles can extract a larger amount of ISF from the skin, and achieve a higher loading capacity with a significant volume change upon insertion[55]. Thirdly, hydrogel microneedles can readily incorporate functional materials to realize specific functions. For instance, GhavamiNejad et al. introduced a continuous glucose monitoring system based on hydrogel microneedles, where they incorporate conductive polymers and nanoparticles to form conductive networks, functioning as working electrodes (Fig. 3d)[55]. Mandal et al. reported a hydrogel microneedle loaded with adjuvants and antigens to monitor skin-resident immunity[54]. Fourthly, adding osmolytes into hydrogel microneedles can further enhance their collection efficiency, attributed to the osmotically driven flow[57]. Lastly, hydrogel microneedles can also serve as reservoirs, necessitating additional procedures to extract the collected ISF from the microneedles[58].

Reverse iontophoresis

The RI method employs an electric voltage to propel positively charged ions through the epidermis, inducing an electroosmotic flow that moves

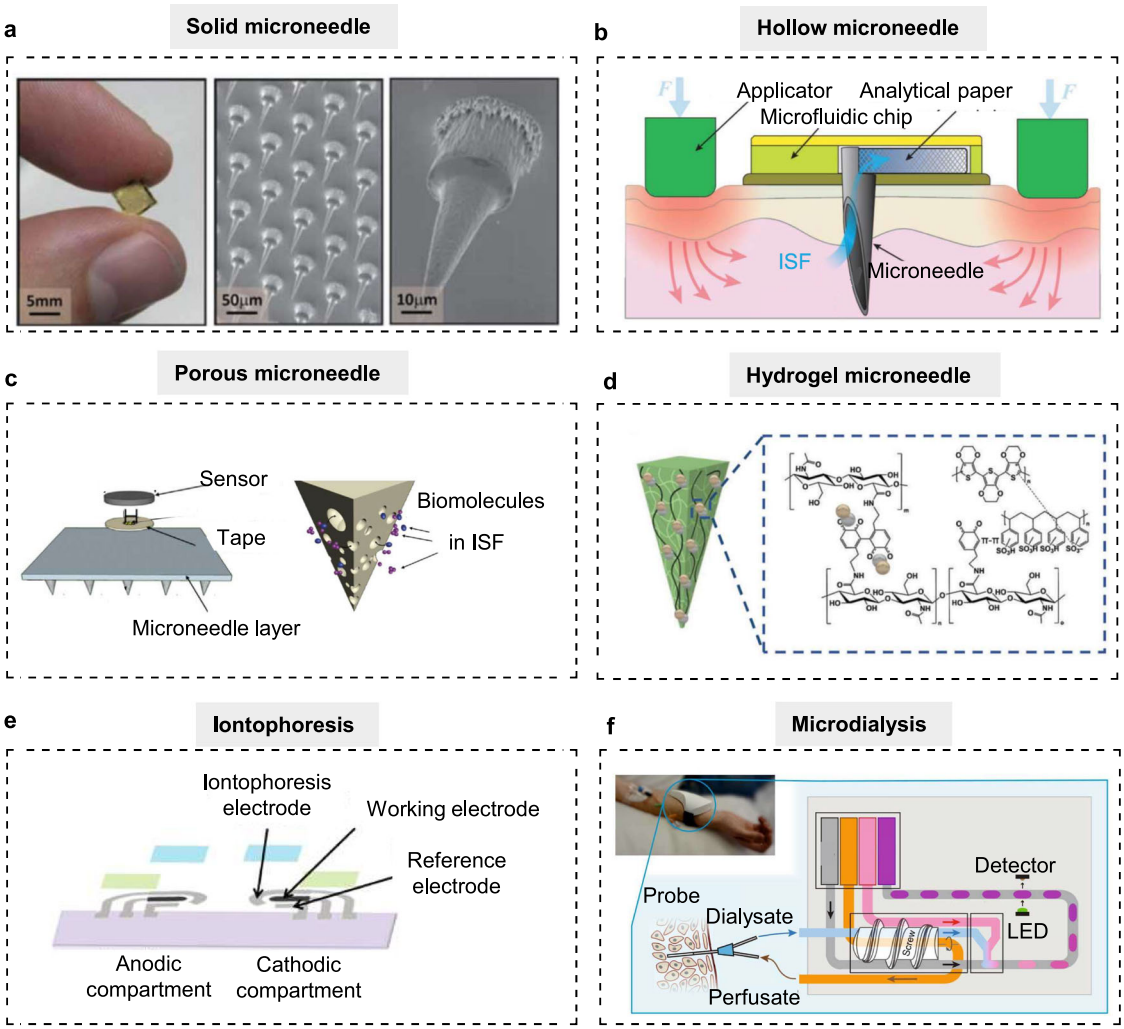

Fig. 3 | ISF sampling techniques. a Functionalized solid microneedle patch for in vivo biomarker detection. Reproduced with permission from ref. [40]., copyright 2011, Royal Society of Chemistry. **b** Hollow microneedle patch for ISF collection that enables multiple analytes detection. Reproduced with permission from ref. [43], copyright 2023, Wiley-VCH. **c** Paper-based porous microneedle patch for pre-diabetes screening test. Reproduced with permission from ref. [51], copyright 2021, Springer Nature Limited. **d** Conductive hydrogel microneedle array for real-time glucose sensing. Reproduced with permission from ref. [55], copyright 2023, Wiley-VCH. **e** Tattoo-based glucose monitoring sensor integrated with iontophoresis[21]. Reproduced under the CC BY-NC 4.0 license. **f** Microfluidic sensor for biomolecule concentration monitoring combined with microdialysis ISF extraction method[24]. Reproduced under the CC BY-NC 4.0 license.

substances out of the skin. In contrast to microneedles used for ISF extraction, the RI method does not require epidermal penetration to access ISF, rendering it entirely non-invasive. The commercially utilized GlucoWatch employed RI for continuous glucose monitoring in real-time. However, it was eventually withdrawn from the market due to reported issues of irritation resulting from excessive current application. Bandodkar et al. introduced a tattoo-based glucose sensor that also utilized RI for ISF sampling, addressing the previous concerns by employing a significantly lower current density(Fig. 3e). They implemented glucose oxidase modified Prussian Blue transducer for selective amperometric biosensing that requires lower working potential[21]. However, it collects biomarkers in a considerably diluted manner, resulting in the extraction of a lower level of biomarkers[4].

Microdialysis

Microdialysis is a relatively invasive method for ISF collection, requiring the insertion of a microdialysis catheter equipped with a semipermeable membrane into the skin. Small analytes in the ISF undergo exchange with the fluid contained within the semipermeable membrane, after which the fluid is transported outside of the skin for subsequent analysis. The microdialysis device can be implanted in vivo for extended durations, from hours to days or even weeks, depending on the specific application requirements. Nightingale et al. combined the microdialysis method with a microfluidic device to enable in situ glucose detection using wet-chemical assays (Fig. 3f)[24]. However, ISF collected through microdialysis typically exhibits a dilution factor of 5–10 times compared to the actual ISF composition[59]. This characteristic renders it less practical for biosensing applications when compared to alternative methods.

Recognizing and sensing mechanisms for ISF analytes

ISF small molecular sensing

Small molecule sensing in ISF majorly relies on electrochemical or optical analysis that transduces concentration information to quantifiable signals through biological or artificial recognition elements. The signals are further processed to withdraw concentration information. Depending on the categories of molecules, different strategies are implemented to maximize transducing efficiency and therefore achieve better sensitivities.

Small molecules. Small molecules can be detected by enzymatic and nonenzymatic methods. Some of the metabolic molecules, such as lactate, glucose, and uric acids, have various enzymes derived from bacteria that can catalyze redox reactions through either flavin adenine dinucleotide

(FAD) or nicotinamide adenine dinucleotide (NADH) redox couple[60,61]. Either through detecting byproducts of the enzymatic reactions or through a redox mediator that facilitates electron transfer between the enzyme's redox cores and electrodes, chemical concentration is correlated with the electron density on the surface of the electrode (Fig. 4a). Commonly used enzymes are oxidases, such as glucose/lactate/alcohol oxidase, which oxidize target molecules and produce hydrogen peroxide (H_2O_2) as byproducts. If H_2O_2 is quantified, platinum nanoparticle[62,63], Prussian blue[64], and horseradish peroxidase[65] are used to improve the efficiency of H_2O_2 decomposition to achieve better sensitivity. If the redox mediator is used, ferrocene[66,67] and other transition metal-based complexes[68] can be included to accept electrons coming from enzymes. Both methods record current change by applying a suitable potential to the electrodes. Though enzymatic reactions are reversible and specific, realizing the long-term stability of both enzyme and redox mediators is challenging and requires careful engineering of functional layers, including film composition, thickness, and homogeneity.

Another category of small metabolic molecules, such as uric acid[69] and dopamine[70], can be detected nonenzymatically through direct electrochemical reactions. In this case, voltammetry techniques (Fig. 4b), such as cyclic voltammetry (CV), square wave voltammetry (SWV), and differential pulse voltammetry (DPV), are utilized to quantify the concentrations via current peak height, which is directly related to the faradic current generated by electrochemical reaction near the electrode's surface[71]. Though such techniques are reagentless and recyclable, their specificity and detection limits are relatively poor when pristine electrodes are used. Electrode surface modification or coupling with low dimensional materials such as graphene[72,73] and carbon nanotube[74] can be implemented to increase the surface area and facilitate electron exchange between target species and electrodes.

Alternatively, optical methods that use target-responsive materials, majorly functional hydrogels[75] or polymer matrix with responsive elements[68,76], can be implemented to semi-quantify the concentration. Fluorescence change in terms of intensity or wavelength shift is measured upon binding of targets (Fig. 4c). However, the fluorescence method usually suffers from poor resolution in quantifying low-concentration molecules and specificity. Instead, surface-enhanced Raman spectroscopy (SERS) can be used to improve the sensitivity and the selectivity over large amounts of interference can be eliminated[77].

Other small molecules, such as amino acids, cortisol, and neurotransmitters, are relatively difficult to sense due to the lack of suitable biological recognition elements, inherent reactivity, and their scarcity of ISF. However, some artificial receptors, such as molecular imprinted polymers (MIP)[14,78,79] (Fig. 4d) and DNA/RNA oligomers[15,17,42,80] (Fig. 4e), are developed to specifically capture those molecules. Usually, a redox-activable label is incorporated into the receptors to transduce the signal. Once the targeted species enter the binding site of these receptors, conformational changes are induced. Such changes are subsequently reflected in the alteration of peaks in redox mediator signals during voltammetry scans. Owing to the high binding affinity between the receptors and targets, ultrahigh-resolution can be achieved (down to pM level) but the signals are usually logarithmically increased, which hinders its sensitivity at large concentrations. Nonetheless, most of the binding is irreversible, which hinders its applications in long-term and continuous monitoring.

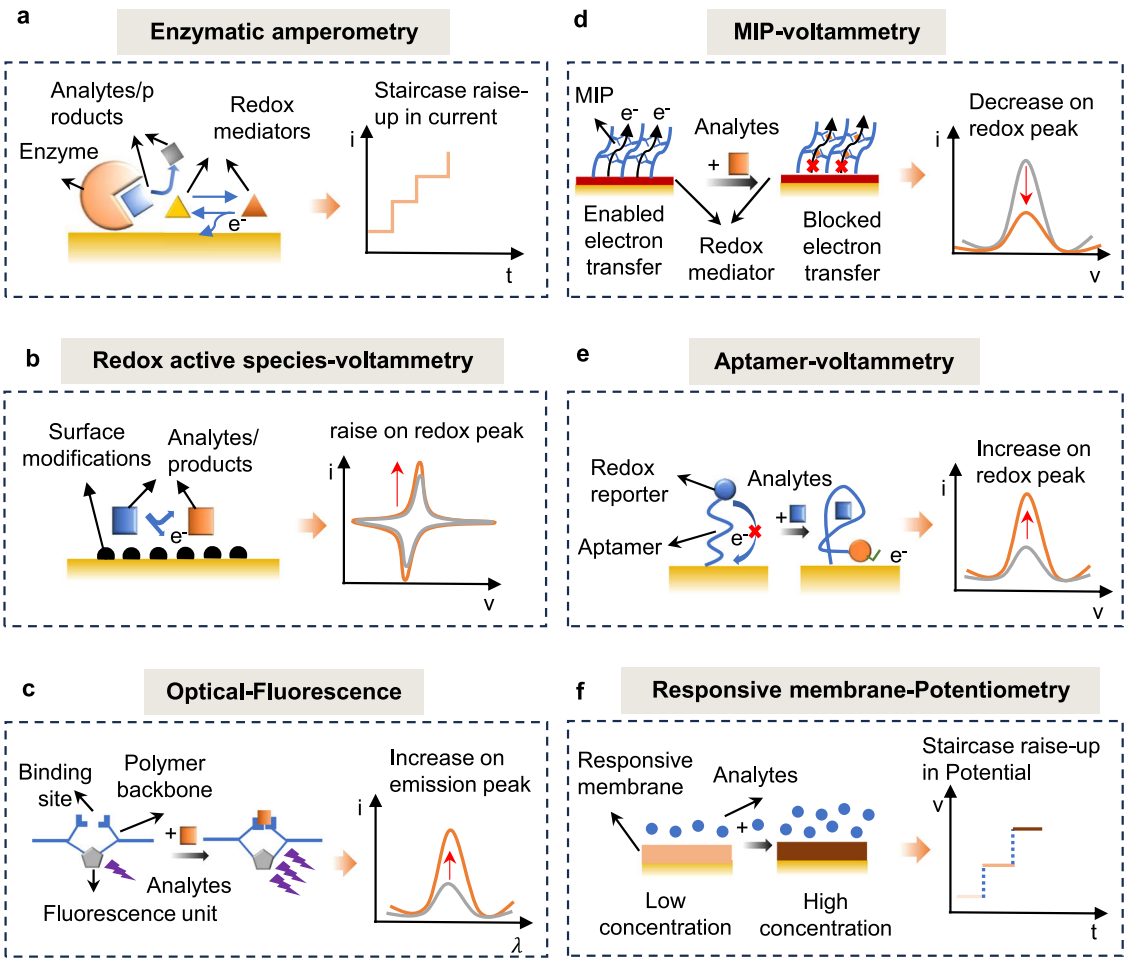

Fig. 4 | Recognizing and sensing mechanisms. a Enzymatic amperometry. **b** Direct redox reaction-based voltammetry sensing. **c** Fluorescence sensing mechanisms. **d** MIP-based voltammetry sensing. **e** Aptamer-based voltammetry sensing. **f** Ion-responsive membrane-based sensing using potentiometry.

Ions and electrolytes. Along with metabolic species, ions and electrolytes are also crucial biomarkers for disease diagnosis (chloride ions for cystic fibrosis) and bacterial infection screening (pH). Most of the ions are measured using open circuit potential (Fig. 4f) with the help of ion-selective membranes, such as sodium ionophore X[12,18,81] and ammonium ionophore I[82]. Potential versus an external reference electrode is evaluated and the signals depend on the ion concentration. For pH sensors, polyaniline (PANi)[83] and Iridium oxides (IrOx)[84] are widely used as both substances appear in different chemical states under different hydrogen ion concentrations, therefore causing a change in charge density. Most of the pH sensors have a sensitivity of around 59 mV/pH, governed by the Nernst equation[85], which predicts the theoretical potential change in a chemical reaction.

ISF macromolecular sensing

Molecules with large molecular weights, such as proteins and polysaccharides, are usually complicated and possess higher dimension structures, preventing any form of direct analysis. Traditional methods of recognizing and sensing mostly rely on antigen-antibody interactions that provide both sensitivities and specificity. Enzyme-linked immunosorbent assay (ELISA) is the most used approach to quantify protein concentrations. Optical signals, like wavelength shift[86], chemiluminescence[87], and fluorescence intensity changes[88], are linked with the presence of molecules. Some amplifying methods such as localized surface plasmonic resonance[89] that uses noble metal colloids (nanorods, nanoparticles) are implemented to improve the sensitivity up to the femtomole level. However, owing to the complicated preparation steps that involve multiple solutions and the harsh requirements of imaging systems, the application of this method on ISF-based monitoring is limited. Some alternative approaches that involve electrochemical transducing are developed to better fit into the existing electronic technologies. Redox-activable antibody[16] and aptamer[90]-based methods are reported to quantify C-active proteins and cytokines.

Sensors and applications

Glucose monitoring

Integrations of sensors with different ISF sampling methods create various platforms that can achieve real-time monitoring of endogenous molecules. Among them, glucose is the most examined molecule as the acquired information could help monitor the progression of diabetes, one of the most prevalent chronic diseases, and offer proper management measures to prevent its deterioration. Several microneedle and RI-based platforms are proposed to serve as a minimally invasive approach to evaluate glucose concentration. Most of them utilized glucose oxidase-based amperometry, which relates concentration information with the change of current as a detection mechanism. For instance, Dervisevic et al. recently proposed a silicon-based high-density microneedle array that successfully detected increasing glucose in mice, proving that the device can penetrate through the skin barrier to assess ISF (Fig. 5a)[91]. Furthermore, Tehrani et al. integrated Poly(methyl methacrylate (PMMA)-based glucose/lactate/alcohol sensors with signal capturing and wireless transmission units in a coin-size wearable device (Fig. 5b)[25]. Human pilot studies indicated that the sensors were able to track events resulting in a rise and fall in glucose levels (e.g. during consumption of meals and snacks) for more than 6 hours. Results correlate well with that of the gold standard finger-prick test with a mean absolute relative difference of 8.83%. Similar strategies were utilized by Yang et al., who fabricated a Polyethylene Terephthalate (PET)-based microneedle glucose sensor (Fig. 5c) that can be inserted into the skin with the help of hollow microneedles[45]. The whole device contains wireless transmission modules and can serve as an alternative to commercialized continuous glucose monitoring devices, such as Freestyle Libres by Abbott. Swellable microneedles are also used to transport sampled ISF to the sensing chamber for further electrochemical measurements (Fig. 5d)[50,57]. In addition, if glucose-responsive materials are used to fabricate needle tips, colorimetric[92], chemiluminescent[93], and florescence[26] signals can be recorded to semi-quantify the glucose concentration. Such methodologies can also be applied to other small molecules, such as uric acid and vitamin C[94].

Though microneedle is an efficient and less invasive platform for transdermal monitoring of ISF, its consistency on penetration depth and sensor stability is hard to control. RI-based patch sensors, on the other hand, only involve planar patterning of functional materials and the ISF sampling rate and amount can be controlled by current density applied. The design of the patch usually consists of a pair of electrodes serving as a direct current (DC) source to induce current flow. Multiple platforms that combine sensors and RI units have been developed. For instance, Pu et al. proposed an all-inkjet-printing patch (Fig. 5e) that included a Na^+ ion differential calibration and a thermal activation unit, which combined to eliminate sweat and temperature interference[95]. To facilitate skin conformation and sensitivity, Chen et al. utilized transfer printing techniques to fabricate an ultrathin nanotextured device that is less than 50 μm and achieves excellent sensitivity at micromole-level of glucose (Fig. 5f)[96]. However, the DC must be applied for several minutes before every single measurement, which means the sampling rate is limited by the nature of the technology. To mitigate this drawback, some researchers combined both microneedles and RI to reduce the ISF collection time and improve the reliability of the sampled ISF composition. Cheng et al. designed a system that consisted of a touch-actuated microneedle RI platform for glucose monitoring, which improved the glucose withdrawing flux by around 1.6 times[34]. Other than solid microneedle, Li et al. utilized a porous microneedle instead to further facilitate the flux of ISF into the sensing chamber, achieving three times than the free diffusion[23]. Though various forms of sensors and devices were developed aiming at continuously measuring glucose in a minimally invasive way, few have conducted rigorous human trials to prove their accuracy. Systematic clinical trials that compare the sensor's readout with the gold standard (YSI 2000 series) are needed to further determine their true effectiveness.

Other metabolic molecules monitoring

Other metabolic biomarkers can also be detected using the above-mentioned methods to help diagnose and monitor diseases such as gout[97], severe diabetes ketoacidosis[98], and phenylketonuria[99]. Ketone bodies were successfully measured in ISF using hollow microneedles that have sensing materials on their cavities[100] (Fig. 6a). A combination of β-hydroxybutyrate dehydrogenase and nicotinamide adenine dinucleotide (NAD +) was used to sense the precursors of ketone bodies. Real-time and stable concentration information is detected. Uric acids, biomarkers that are derived from purine metabolisms, can accumulate in their crystal form in joints and cause gout. Zhang et al.[94] reported a colorimetric microneedle sensor based on uricase and a 3,3′,5,5′-tetramethylbenzidine (TMB) system (Fig. 6b). H_2O_2 generated by uricase reacted with TMB to create a change in color and the linear detection range was determined as 200–1000 μM. Though successfully demonstrated on porcine skin with different uric acid concentrations, missing in vivo data weakens the significance of this work. Lactate was also measured in ISF though most of the work focused on sweat lactate concentration detection. ISF lactate concentration is much more accurate than that of sweat due to sweat's dilution effect[101]. Sensors had been proposed to access ISF lactate concentration for monitoring anaerobic metabolism and muscle conditions. The sampling methods as well as detection mechanisms are similar to that of glucose sensors. Microneedle[102,103] and RI[104] (Fig. 6c) were used to sample ISF, and lactate oxidase is the recognition element utilizing similar sensing mechanisms as the glucose sensor. In vitro experiments demonstrated the capability of dynamic monitoring but like its counterpart glucose, systematic evaluations in humans regarding its accuracy are still at the early stage.

Nutrients, unlike metabolic molecules that have strong correlations with diseases, can be used to prevent and manage nutritional imbalance. One example is to use the most common vitamin, vitamin C, as the biomarker to track the daily balance of nutrient intake. Unlike the common method that directly measures vitamin C through its oxidizing properties, Sempionatto et al.[105] designed a stretchable RI patch (Fig. 6e) that

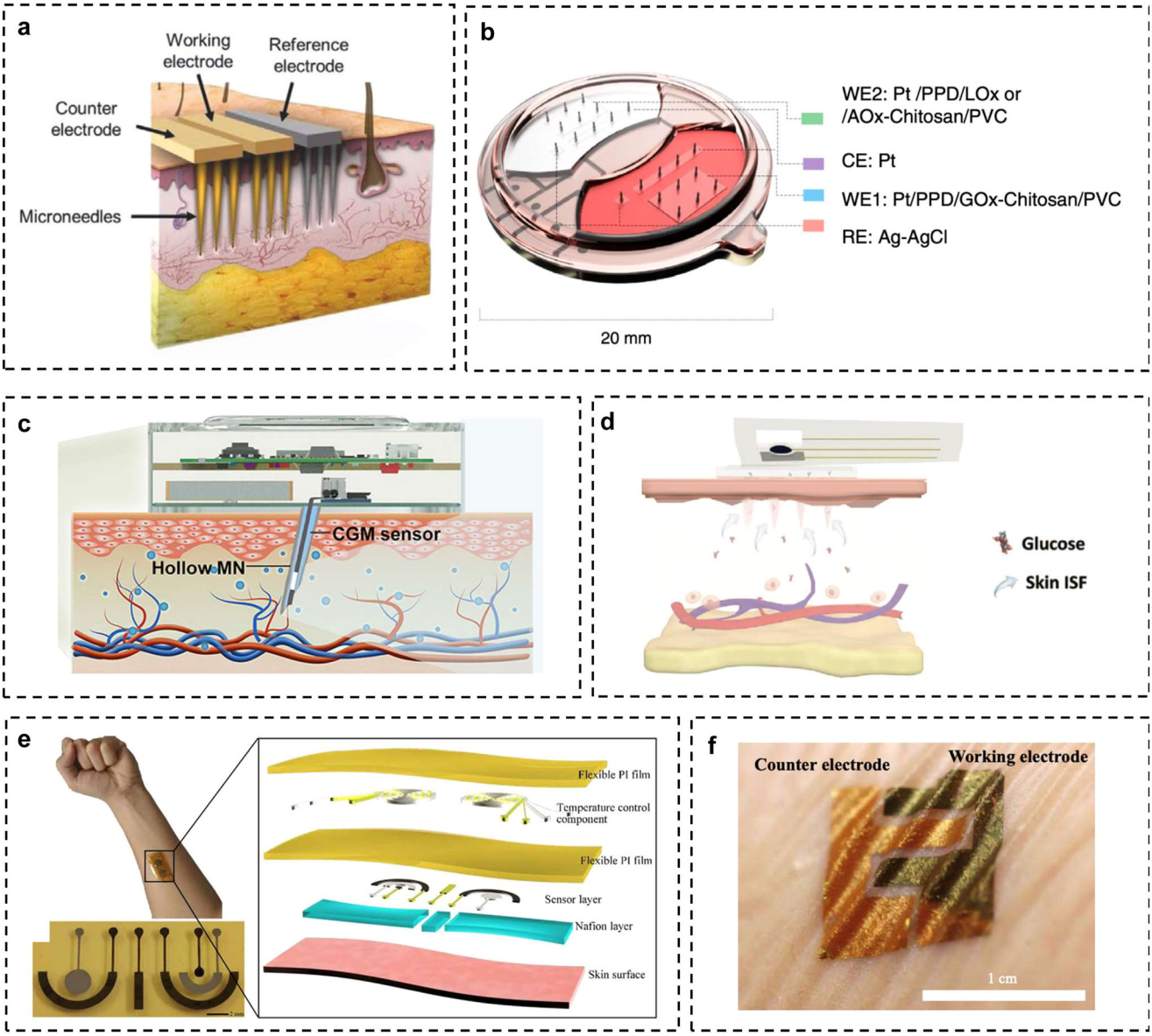

Fig. 5 | ISF glucose sensing. a Illustration of high-density microneedle-based glucose sensor. Reproduced with permission from ref. [91], copyright 2021, Wiley-VCH. **b** Illustration of integrated PMMA-based microneedle electrochemical sensors. Reproduced with permission from ref. [25], copyright 2022, Springer Nature Limited. **c** Schematic illustration of PET-based continuous glucose sensor for diabetes management. Reproduced with permission from ref. [45], copyright 2023, American Chemical Society. **d** Schematic illustration of a swellable microneedle-based glucose sensor. Reproduced with permission from ref. [57], copyright 2021, Wiley-VCH. **e** Optical and layer-by-layer illustration of RI-based patch glucose sensor[95]. Reproduced under the CC BY-NC 4.0 license. **f** Optical image of RI-based ultrathin glucose sensor[96]. Reproduced under the CC BY-NC 4.0 license.

immobilized ascorbate oxidase to enable continuous measurement with high specificity. Human trials involving the intake of different doses of vitamin C tablets were performed to validate the ability of the sensors to reflect the instant change in vitamin C levels in the human body. A similar approach was also adopted by Zhao et al.[106] (Fig. 6d), who utilized similar recognition mechanisms but integrated the sensor with a wireless system and achieved long-term monitoring for more than a day. Other nutrients such as amino acids[14] and caffeine[107] offer useful information to track diets and overall body conditions. However, all existing literatures focus on sweat analysis with very few focusing on ISF.

pH and electrolyte monitoring

Electrolytes consist of various elemental ions, such as sodium (Na^+), potassium (K^+), zinc (Zn^{2+}), and chloride (Cl^-) ions, which exist in our body to serve critical roles, such as maintaining the stable chemical condition of biofluids, electrical potentials across the cell membranes, and even some acting as biomarkers of diseases. Na^+ and K^+ can be not only viewed as reference biomarkers for overall electrolyte concentration but also related to hypertension and cardiovascular diseases. As such, devices have been developed to assess their concentrations precisely and continuously. Since the RI approach needs electrical stimulation, the composition of stimulated ISF will be affected by the electroosmotic process[3], resulting in an aggregation of those species at cathodes. Therefore, microneedle-based methods are commonly used to assess Na^+ and K^+ concentrations in ISF. A hollow microneedle (Fig. 6f) that had K^+ and Na^+-sensitive electrodes inserted was introduced to simultaneously measure the two ions[108]. A porous microneedle coupled with flat screen printed sodium sensing electrode was also reported with pilot human trials data to prove its feasibility as a monitoring tool[109]. One step further, a solid microneedle sensor array (Fig. 6g) that can measure multiple ions (Na^+, K^+, Cl^-, lithium (Li^+), calcium (Ca^{2+})) was developed and validated in vivo[110]. All of them utilize the potentiometry technique, which relies on the chemical potential shift of the ion-sensitive

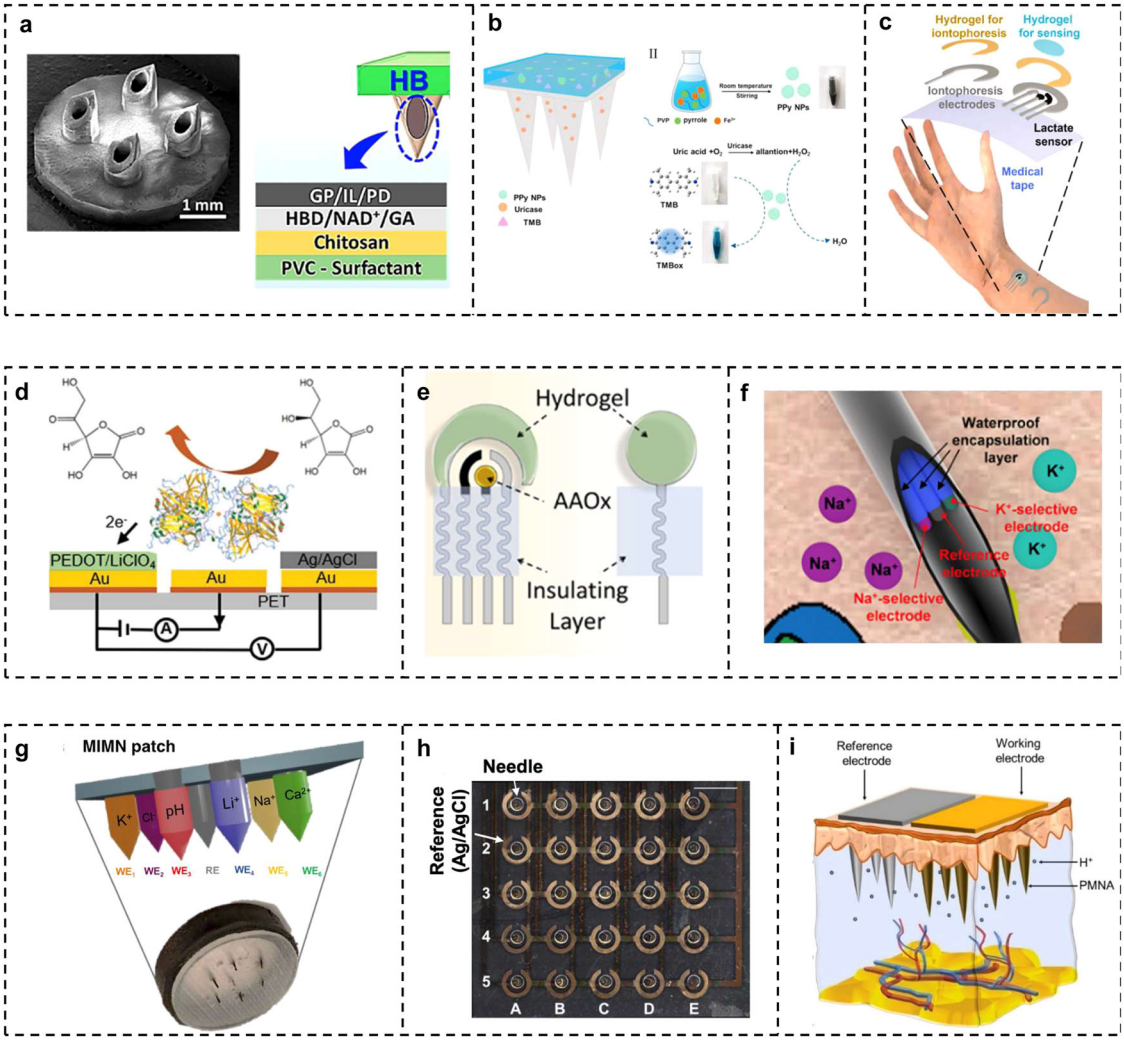

Fig. 6 | ISF sensors for the detection of other small molecules. a SEM image and layer-by-layer illustration of ketone bodies sensor. Reproduced with permission from ref. [100], copyright 2020, American Chemical Society. **b** Colorimetric uric acid sensor and its mechanism. Reproduced with permission from ref. [94], copyright 2023, Elsevier. **c** Structural illustration of wearable lactate sensor that quantifies ISF lactate concentration. Reproduced with permission from ref. [104], copyright 2023, Elsevier. **d** Structure illustration and sensing mechanism of the wearable ascorbic acid sensor, reproduced with permission from ref. [106], copyright 2020, Wiley-VCH. **e** Structure illustration of stretchable vitamin C sensor, reproduced with permission from ref. [105], copyright 2020, American Chemical Society. **f** Illustration of the device configuration of Na^+, K^+ sensor inserted into the hollow microneedle, reproduced with permission from ref. [108], copyright 2020, American Chemical Society. **g** Optical and illustration images of multiple ions microneedle-based sensor from ref. [110], Reproduced under the CC BY 4.0 license. **h** Conformable pH sensors array with the ability of mapping[111]. Reproduced under the CC BY-NC 4.0 license. **i** Illustration of high-density microneedle-based pH sensor. Reproduced with permission from ref. [112], copyright 2023, Elsevier.

membrane on the electrodes when encountering different concentrations of targets. Potential signals can then be transmitted to smartphones for analysis and recording purposes. To facilitate wearability, stretchable microneedle patches can be investigated.

pH is another important characteristic of human health. Abnormal pH in biofluids and certain regions of bodies such as limbs usually indicates an underlying disease. Since ISF is directly diffused from the blood circulation, its ability to reflect a systematic change of chemical condition is better than sweat, which is secreted by the eccrine glands. The absence of epidermal chemical interferences and bacteria metabolites also makes ISF a better candidate for withdrawing pH information over sweat. Various forms of pH sensors have been developed. For instance, Lee et al. utilized a conformable microneedle array to measure the regional pH level of limbs (Fig. 6h)[111]. pH mapping of 25 separate regions was achieved and successfully captured pH change in regions affected by periphery artery diseases. Dervisevic et al. also reported a high-density microneedle array with a higher sensitivity of 62.9 mV pH^{-1} for an enlarged detection area (Fig. 6i)[112]. Though the change in ISF pH can be detected through the aforementioned technologies, its in vivo long-term monitoring is seldom reported. The possible reason can be the long-term stability issues of pH sensors under biological environment[113]. Moreover, the lack of clinical explanation and proven relevance of the local ISF pH alteration with the disease weaken the significance of long-term pH monitoring.

Hormones and proteins monitoring

Hormones, characterized by their diminutive molecular structures, exhibit the capacity to permeate capillary walls and traverse into ISF[114]. Notably, steroid hormones, such as cortisol, often tend to bind with albumin and various protein carriers[115]. As a result, the hormone monitoring shifts from assessing the conventional total concentration to the unbound bioavailable fractions. Generally, ISF-based sensors detect the unbound bioavailable fraction of hormones instead of the total fraction. Cortisol, as a typical hormone, can serve as a crucial indicator of the stress response and play a regulatory role in the immune system. Thus, its detection has gained lots of interest. For instance, Venugopal et al. introduced a real-time cortisol monitoring device based on electrochemical impedance spectroscopy and, for the first time, investigated the correlation of cortisol levels between ISF

and plasma[116]. They extracted ISF through micropores created by a near-infrared laser. Subsequently, electrode patches functionalized with dithiobis were employed to detect cortisol in ISF, enabling continuous monitoring of cortisol levels throughout an entire day, including during sleep.

Cytokines are small proteins responsible for regulating the activities and functions of immune cells and blood cells. Monitoring cytokines in ISF can be instrumental in detecting and understanding immune responses. At the onset of an immune response, a substantial number of cytokines are released within a brief timeframe, a phenomenon often referred to as a "cytokine storm[117]." To offer more comprehensive data for the prompt diagnosis and treatment of patients with inflammation, recent studies have introduced various methods for monitoring cytokines. Xu et al. proposed the first real-time platform to capture and measure proteins in ISF (Fig. 7a)[118]. They introduced functionalized carbon nanotubes to capture cytokines using specific antibodies on the microneedles. Furthermore, rather than detecting cytokines after the removal of microneedle patches, the platform facilitates real-time electrochemical analysis of cytokines by combining cytokine capture and analysis through the electrochemical method. Optical methods are also extensively employed in the detection of cytokines due to their ease of observation. Zhang et al. introduced an innovative approach for the concurrent detection of multiple cytokines, integrating photonic crystal (PhC) barcodes with microneedles (Fig. 7b)[119]. Upon skin penetration by the microneedles, cytokines promptly adhere to the barcode-equipped microneedle tips. Then, they introduced fluorescent probes to form immunocomplexes, enabling the assessment of the relative quantity of cytokines based on the fluorescent intensity of the barcodes. Furthermore, distinct cytokines can be differentiated based on variations in their reflection peaks.

Antibodies are substantial proteins produced by the immune system in response to antigens. Assessing antibody levels is crucial in delivering conclusive information for the early detection of diseases. The concentration of antibodies in ISF is typically around 15–25% of that in the blood[2]. Bao et al introduced a diagnostic platform comprising a porous microneedle patch and immunochromatography, which allowed for the swift detection of anti-SARS-CoV-2 IgM/IgG antibodies (Fig. 7c)[120]. In this study, ISF was collected using a biodegradable porous microneedle patch. Thereafter, ISF was transferred to a paper-based sensor comprising colloidal gold immunoassay for analysis. The test results were then visualized through the color bands on the sensor. Wang et al. performed the monitoring of both cytokines and antibodies with a microneedle patch (Fig. 7d)[121]. The microneedles were functionalized with antibodies to capture specific target biomarkers. Utilizing the principles of ELISA, they implemented a fluorophore-linked immunosorbent assay that notably elevated the detection sensitivity. This innovation resulted in about 800-fold reduction in the detection limit when compared to conventional methods, enabling the achievement of ultra-sensitive and quantitative measurements of protein biomarkers.

Drugs monitoring

Non-invasive drug monitoring has been extensively explored for both therapeutic drugs and recreational drugs, especially illicit addictive drugs. In terms of therapeutic drugs such as levodopa, vancomycin, theophylline, and others, different individuals may necessitate varying drug dosages to achieve optimal therapeutic outcomes[122]. Furthermore, the misuse of recreational drugs, such as opioids and morphine, poses a severe threat to public health and social order. As a result, lots of effort has been put into developing technologies for real-time drug monitoring, ranging from tailoring drug dosages to individual needs to enhancing therapeutic efficacy and controlling the abuse of drugs.

In the case of therapeutic drug monitoring, unlike the blood-based method which usually detects the concentration of drugs that are bound to proteins, ISF-based sensors possess the advantage of exclusively detecting bioavailable drugs that are not bound to proteins and thus, provide a more accurate reflection of the active drug level[123]. Rawson et al. developed the first-in-human, proof-of-concept microneedle-based ISF sensor for monitoring the drug phenoxymethylpenicillin within a healthy human body (Fig. 8a)[124]. This sensor features a working electrode functionalized with iridium oxide to measure changes in pH and a hydrogel layer containing β-lactamase to catalyze diffused phenoxymethylpenicillin into penicillate and a proton. As the concentration of protons increases and pH drops, the sensor gives varied open circuit potential output, which can reflect the concentration of the phenoxymethylpenicillin, showing results in line with the current gold standard microdialysis. To offer more comprehensive information through drug monitoring, Goud et al. integrated tyrosinase-based enzymatic-amperometry and nonenzymatic voltammetry to achieve dual-sensing of L-dopa, ensuring the reliability of acquired concentration

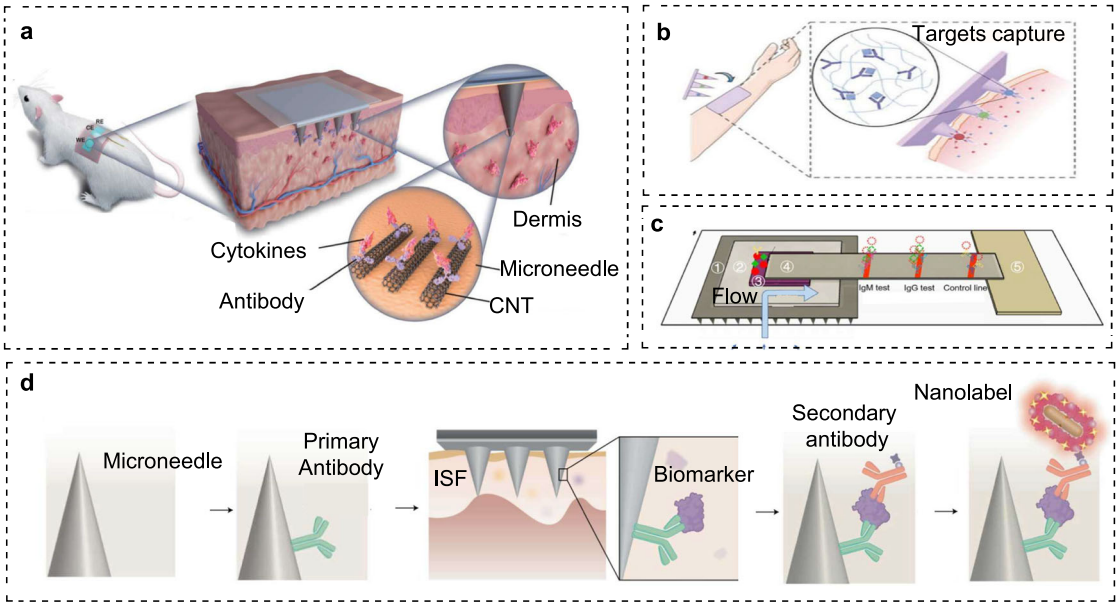

Fig. 7 | ISF macromolecules sensing. a Platform for the capture and measurement of protein in ISF. Reproduced with permission from ref. [118], copyright 2023, Wiley-VCH. **b** Encoded microneedle arrays for optical detection of multiple cytokines. Reproduced with permission from ref. [119], copyright 2019, Wiley-VCH. **c** Porous microneedle patch for swift detection of anti-SARS-CoV-2 IgM/IgG antibodies[120]. Reproduced under the CC BY 4.0 license. **d** Microneedle patch for cytokine and antibody detection. Reproduced with permission from ref. [121], copyright 2021, Springer Nature Limited.

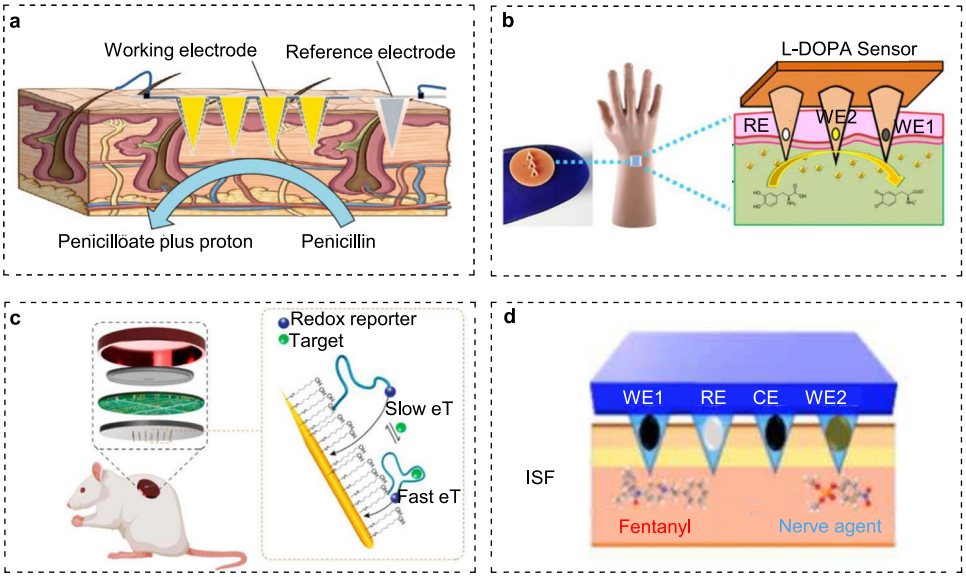

Fig. 8 | ISF drugs monitoring. a Microneedle-based sensor for phenoxymethylpenicillin monitoring[124]. Reproduced under the CC BY 4.0 license. **b** Dual-sensing platform for L-dopa measurement. Reproduced with permission from ref. [44], copyright 2019, American Chemical Society. **c** Microneedle aptamer-based sensor for multi-target measurement[42]. Reproduced under the CC BY-NC-ND 4.0 license. **d** Microneedle-based sensing platform for the measurement of fentanyl and organophosphates. Reproduced with permission from ref. [46], copyright 2020, American Chemical Society.

information (Fig. 8b). This sensing platform offers effective real-time feedback for the measurement of L-dopa, thereby enhancing the informational content available for diagnosis. Nonetheless, the detection based on enzymatic conversion processes via oxidases or reductases, restricts the range of target molecules, while aptamer-based sensors can largely widen the detectable targets. For instance, Wu et al. introduced a microneedle aptamer-based sensor for detecting cancer drugs and antibiotics (Fig. 8c)[42]. In their approach, single-stranded nucleic acid sequences were employed as aptamers, which were selected through the process of Systematic Evolution of Ligands by Exponential Enrichment (SELEX). Therapeutic drugs, including irinotecan, doxorubicin, and tobramycin, were quantified both in vitro and in vivo, showing good real-time sensitivity and compliance with the pharmacokinetic model. These aptamers were engineered to exhibit high-affinity binding to a wide array of target molecules, enabling multi-target measurement with a single platform.

In addition to therapeutic drug monitoring, there is significant interest in continuous monitoring of recreational drugs for abuse prevention. For example, Mishra et al. proposed a microneedle-based ISF sensing platform for the simultaneous measurement of fentanyl and organophosphates (Fig. 8d)[46]. The sensor contains two working electrodes that were customized for the separate detection of fentanyl and organophosphates. This design allowed for the differentiation of opioid overdose from nerve agent poisoning, as both could exhibit similar effects.

Challenges and future direction

ISF sensors exhibit significant potential for diagnosis, managing disease, and monitoring drugs by detecting vital and clinically relevant biomarkers or drugs non-invasively or with minimal invasiveness. These advances may facilitate personalized medicine and point-of-care applications. However, some challenges still exist.

Firstly, longevity and long-term continuous monitoring pose significant issues for many ISF sensors. Currently, small molecule sensors, such as glucose and lactate sensors, have been reported to last for more than 24 hours. A representative example is glucose sensors utilizing robust and selective glucose oxidase. Commercial products such as Abbott's FreeStyle Liber, Dexcom's G4, G5, and G6 Medtronic's Minimed Guardian have been reported to last for more than 7 days. However, at present, only very limited highly analyte-specific and robust enzymes are engineered or discovered for certain targets. Numerous targets lack effective recycling recognizing elements, particularly for macromolecule targets such as proteins whose sensing is based on bio-affinity sensing mechanisms. Bioaffinity sensing involves the binding of targets with aptamers, antibodies, or engineered receptors, whose detachment from recognizing elements is challenging, especially for sensors with high selectivity and sensitivity. Generally, bonded targets gradually accumulate on the sensing surface, leading to ineffectiveness and inaccuracy. Possible solutions that utilized external stimulation to regenerate sensing elements[125] or designed releasing mechanisms were developed, trying to solve the issue.

Secondly, accuracy and reliability also present significant challenges for ISF sensors. In-situ monitoring faces issues such as the accumulation of analytes and byproducts, and biofouling on the sensing sites, interfering with the target recognition and response. Utilizing biocompatible outer coating films[126], zwitterionic membranes[127], or hydrogels[54] can significantly reduce the biofouling problems and avoid perturbing the immune response but will require careful molecule design. Non-in-situ monitoring involving the frequent, continuous, and abundant extraction or transport of ISF to an invitro location, causes localized repelling, and immune effects, and distorts ISF components or concentration. This results in an unreliable correlation between ISF and blood concentration which leads to inaccuracy. Possible solutions involve the development of systems capable of controlling the extracted amount of ISF, as well as the duration and frequency of extraction, ensuring that the amount, duration, and frequency do not trigger significant immune response or distort the target concentration. Additionally, sensitive sensors that require minimal ISF amount can also be explored.

Thirdly, motion strain poses great challenges to the accuracy, reliability, and longevity of wearable ISF sensors as well. While wearable and flexible format brings opportunities for convenience and facile diagnosis, it introduces significant mechanical strains on sensors during human activity. Frequent large strains may cause detachment of the sensing component from the skin and potential physical damage to the sensing components. A flexible substrate that has an engineered strain-insensitive design can partially mitigate this issue by minimizing the interference on the sensor end[62,128,129]. However, the rigid-soft interfaces and poor compatibility of the silicon industry with the commonly used flexible substrates hinder the advancement of the flexible sensor towards commercialization.

Fourthly, achieving ISF sensors with low lag time, fast response time, high sensitivity, and wide sensing range are challenging. Lag time mainly depends on the inherent process of the analytes to pass from blood into ISF (5 – 10 min for small molecules such as glucose) and the time for targets to diffuse from ISF to the electrode surface (1–5 min for glucose sensor with limiting membrane)[2,130] To deal with the time-lag, artificial intelligence, and algorithm-based prediction methods[131,132] may be used to compensate the lag time for more precise measurements. Another possible strategy is to develop a highly efficient membrane that can facilitate the transportation of analytes

to the sensing core while keeping the linear response and biocompatibility performance. Regarding sensitivity and sensing range, better sensing mechanisms and optimized sensing components can be designed to refine the recognition and sensing approaches between the electrodes and targets.

Future works can focus on long-term reliable and accurate sensing, especially for the macromolecules, such as cytokines, cortisol, and proteins. Advances in ISF-based sensing have the potential to revolutionize personalized diagnosis and medicine, particularly in immune system-related diseases. Moreover, there is a need for more biochemical and physically robust sensing membranes capable of withstanding complex biological environments and human activity. Developing anti-biofouling and strain-insensitive functional membranes is essential. Finally, further in vivo studies comparing sensor-detected ISF concentrations to those in the blood are needed to bolster confidence in the use of ISF for biosensing applications.

Received: 6 December 2023; Accepted: 27 February 2024;
Published online: 13 March 2024

References

1. Fogh-Andersen, N., Altura, B. M., Altura, B. T. & Siggaard-Andersen, O. Composition of interstitial fluid. *Clin. Chem.* **41**, 1522–1525 (1995).
2. Heikenfeld, J. et al. Accessing analytes in biofluids for peripheral biochemical monitoring. *Nat. Biotechnol.* **37**, 407–419 (2019).
3. Friedel, M. et al. Opportunities and challenges in the diagnostic utility of dermal interstitial fluid. *Nat. Biomed. Eng.* **7**, 1–15 (2023).
4. Kim, Y. & Prausnitz, M. R. Sensitive sensing of biomarkers in interstitial fluid. *Nat. Biomed. Eng.* **5**, 3–5 (2021).
5. Samant, P. P. et al. Sampling interstitial fluid from human skin using a microneedle patch. *Sci. Transl. Med.* **12**, eaaw0285 (2020).
6. Frank, R. & Hargreaves, R. Clinical biomarkers in drug discovery and development. *Nat. Rev. Drug Discov.* **2**, 566–580 (2003).
7. Samant, P. P. & Prausnitz, M. R. Mechanisms of sampling interstitial fluid from skin using a microneedle patch. *Proc. Natl Acad. Sci. USA* **115**, 4583–4588 (2018).
8. Kim, J. et al. Wearable smart sensor systems integrated on soft contact lenses for wireless ocular diagnostics. *Nat. Commun.* **8**, 14997 (2017).
9. Moreddu, R., Wolffsohn, J. S., Vigolo, D. & Yetisen, A. K. Laser-inscribed contact lens sensors for the detection of analytes in the tear fluid. *Sens. Actuat. B: Chem.* **317**, 128183 (2020).
10. Kim, J. et al. Wearable salivary uric acid mouthguard biosensor with integrated wireless electronics. *Biosens. Bioelectron.* **74**, 1061–1068 (2015).
11. García-Carmona, L. et al. Pacifier biosensor: toward noninvasive saliva biomarker monitoring. *Anal. Chem.* **91**, 13883–13891 (2019).
12. Gao, W. et al. Fully integrated wearable sensor arrays for multiplexed in situ perspiration analysis. *Nature* **529**, 509–514 (2016).
13. Mukasa, D. et al. A computationally assisted approach for designing wearable biosensors toward non-invasive personalized molecular analysis. *Adv. Mater.* **35**, 2212161 (2023).
14. Wang, M. et al. A wearable electrochemical biosensor for the monitoring of metabolites and nutrients. *Nat. Biomed. Eng.* **6**, 1225–1235 (2022).
15. Lin, S. et al. Wearable microneedle-based electrochemical aptamer biosensing for precision dosing of drugs with narrow therapeutic windows. *Sci. Adv.* **8**, eabq4539 (2022).
16. Tu, J. et al. A wireless patch for the monitoring of C-reactive protein in sweat. *Nat. Biomed. Eng.* **7**, 1293–1306 (2023).
17. Ye, C. et al. A wearable aptamer nanobiosensor for non-invasive female hormone monitoring. *Nat. Nanotechnol.* https://doi.org/10.1038/s41565-023-01513-0 (2023).
18. Zheng, Y. et al. A wearable microneedle-based extended gate transistor for real-time detection of sodium in interstitial fluids. *Adv. Mater.* **34**, 2108607 (2022).
19. Yang, B., Kong, J. & Fang, X. Programmable CRISPR-Cas9 microneedle patch for long-term capture and real-time monitoring of universal cell-free DNA. *Nat. Commun.* **13**, 3999 (2022).
20. Yang, J. et al. Masticatory system–inspired microneedle theranostic platform for intelligent and precise diabetic management. *Sci. Adv.* **8**, eabo6900 (2022).
21. Bandodkar, A. J. et al. Tattoo-based noninvasive glucose monitoring: a proof-of-concept study. *Anal. Chem.* **87**, 394–398 (2015).
22. Yao, Y. et al. Integration of interstitial fluid extraction and glucose detection in one device for wearable non-invasive blood glucose sensors. *Biosens. Bioelectron.* **179**, 113078 (2021).
23. Li, X. et al. A fully integrated closed-loop system based on mesoporous microneedles-iontophoresis for diabetes treatment. *Adv. Sci.* **8**, 2100827 (2021).
24. Nightingale, A. M. et al. Monitoring biomolecule concentrations in tissue using a wearable droplet microfluidic-based sensor. *Nat. Commun.* **10**, 2741 (2019).
25. Tehrani, F. et al. An integrated wearable microneedle array for the continuous monitoring of multiple biomarkers in interstitial fluid. *Nat. Biomed. Eng.* **6**, 1214–1224 (2022).
26. Sang, M. et al. Fluorescent-based biodegradable microneedle sensor array for tether-free continuous glucose monitoring with smartphone application. *Sci. Adv.* **9**, eadh1765 (2023).
27. McGrath, J., Eady, R. & Pope, F. Anatomy and organization of human skin. *Rook's Textbook of Dermatol.* **1**, 3.2–3.80 (2004).
28. Brinkman, J. E., Dorius, B. & Sharma, S. Physiology, body fluids. Treasure Island (FL): StatPearls Publishing. https://europepmc.org/article/NBK/nbk482447 (2023)
29. Mehta, D. & Malik, A. B. Signaling mechanisms regulating endothelial permeability. *Physiol. Rev.* **86**, 279–367 (2006).
30. Haaverstad, R., Romslo, I., Larsen, S. & Myhre, H. Protein concentration of subcutaneous interstitial fluid in the human leg: a comparison between the wick technique and the blister suction technique. *Int. J. Microcircul.* **16**, 111–117 (1996).
31. Rippe, B. & Haraldsson, B. Transport of macromolecules across microvascular walls: the two-pore theory. *Physiol. Rev.* **74**, 163–219 (1994).
32. Egawa, G. et al. Intravital analysis of vascular permeability in mice using two-photon microscopy. *Sci. Rep.* **3**, 1932 (2013).
33. Yang, B., Fang, X. & Kong, J. Engineered microneedles for interstitial fluid cell-free DNA capture and sensing using iontophoretic dual-extraction wearable patch. *Adv. Funct. Mater.* **30**, 2000591 (2020).
34. Cheng, Y. et al. A touch-actuated glucose sensor fully integrated with microneedle array and reverse iontophoresis for diabetes monitoring. *Biosens. Bioelectron.* **203**, 114026 (2022).
35. Vermeer, B. J., Reman, F. C. & van Gent, C. M. The determination of lipids and proteins in suction blister fluid. *J. Investig. Dermatol.* **73**, 303–305 (1979).
36. Rossing, N. & Worm, A. M. Interstitial fluid: exchange of macromolecules between plasma and skin interstitium. *Clin. Physiol.* **1**, 275–284 (1981).
37. Gebhart, S. et al. Glucose sensing in transdermal body fluid collected under continuous vacuum pressure via micropores in the stratum corneum. *Diabetes Technol. Therap.* **5**, 159–166 (2003).
38. Saha, T. et al. Wearable electrochemical glucose sensors in diabetes management: a comprehensive review. *Chem. Rev.* **123**, 7854–7889 (2023).
39. Aldawood, F. K., Andar, A. & Desai, S. A comprehensive review of microneedles: types, materials, processes, characterizations and applications. *Polymers* **13**, 2815 (2021).
40. Corrie, S. R. et al. Surface-modified microprojection arrays for intradermal biomarker capture, with low non-specific protein binding. *Lab on a Chip* **10**, 2655–2658 (2010).

41. Liu, Y., Yu, Q., Luo, X., Yang, L. & Cui, Y. Continuous monitoring of diabetes with an integrated microneedle biosensing device through 3D printing. *Microsyst. Nanoeng.* **7**, 75 (2021).
42. Wu, Y. et al. Microneedle aptamer-based sensors for continuous, real-time therapeutic drug monitoring. *Anal. Chem.* **94**, 8335–8345 (2022).
43. Ribet, F. et al. Microneedle patch for painless intradermal collection of interstitial fluid enabling multianalyte measurement of small molecules, SARS-CoV-2 antibodies, and protein profiling. *Adv. Healthc. Mater.* **12**, 2202564 (2023).
44. Goud, K. Y. et al. Wearable electrochemical microneedle sensor for continuous monitoring of levodopa: toward Parkinson management. *ACS sensors* **4**, 2196–2204 (2019).
45. Yang, J. et al. Development of smartphone-controlled and microneedle-based wearable continuous glucose monitoring system for home-care diabetes management. *ACS sensors* **8**, 1241–1251 (2023).
46. Mishra, R. K. et al. Continuous opioid monitoring along with nerve agents on a wearable microneedle sensor array. *J. Am. Chem. Soc.* **142**, 5991–5995 (2020).
47. Mishra, R. K., Mohan, A. V., Soto, F., Chrostowski, R. & Wang, J. A microneedle biosensor for minimally-invasive transdermal detection of nerve agents. *Analyst* **142**, 918–924 (2017).
48. Liu, G.-S. et al. Microneedles for transdermal diagnostics: Recent advances and new horizons. *Biomaterials* **232**, 119740 (2020).
49. Gao, G., Zhang, L., Li, Z., Ma, S. & Ma, F. Porous microneedles for therapy and diagnosis: fabrication and challenges. *ACS Biomater. Sci. Eng.* **9**, 85–105 (2022).
50. Kusama, S. et al. Transdermal electroosmotic flow generated by a porous microneedle array patch. *Nat. Commun.* **12**, 1–11 (2021).
51. Lee, H. et al. Porous microneedles on a paper for screening test of prediabetes. *Med. Devices Sens.* **3**, e10109 (2020).
52. Kai, H. & Kumatani, A. A porous microneedle electrochemical glucose sensor fabricated on a scaffold of a polymer monolith. *J. Phys.: Energy* **3**, 024006 (2021).
53. Zhang, X., Wang, Y., Chi, J. & Zhao, Y. Smart microneedles for therapy and diagnosis. *Research (Wash D C)* **2020**, 7462915 (2020).
54. Mandal, A. et al. Cell and fluid sampling microneedle patches for monitoring skin-resident immunity. *Sci. Transl. Med.* **10**, eaar2227 (2018).
55. GhavamiNejad, P. et al. A conductive hydrogel microneedle-based assay integrating PEDOT: PSS and Ag-Pt nanoparticles for real-time, enzyme-less, and electrochemical sensing of glucose. *Adv. Healthc. Mater.* **12**, 2202362 (2023).
56. Donnelly, R. F. et al. Hydrogel-forming microneedle arrays for enhanced transdermal drug delivery. *Adv. Funct. Mater.* **22**, 4879–4890 (2012).
57. Zheng, M. et al. Osmosis-powered hydrogel microneedles for microliters of skin interstitial fluid extraction within minutes. *Adv. Healthcare Mater.* **9**, 1901683 (2020).
58. Chang, H. et al. A swellable microneedle patch to rapidly extract skin interstitial fluid for timely metabolic analysis. *Adv. Mater.* **29**, 1702243 (2017).
59. Korf, J., Huinink, K. D. & Posthuma-Trumpie, G. A. Ultraslow microdialysis and microfiltration for in-line, on-line and off-line monitoring. *Trends Biotechnol.* **28**, 150–158 (2010).
60. Wilson, R. & Turner, A. P. F. Glucose oxidase: an ideal enzyme. *Biosens. Bioelectron.* **7**, 165–185 (1992).
61. Ferri, S., Kojima, K. & Sode, K. Review of glucose oxidases and glucose dehydrogenases: a bird's eye view of glucose sensing enzymes. *J. Diabetes Sci. Technol.* **5**, 1068–1076 (2011).
62. Zhao, Y. et al. A wearable freestanding electrochemical sensing system. *Sci. Adv.* **6**, eaaz0007 (2020).
63. Zhai, D. et al. Highly sensitive glucose sensor based on Pt nanoparticle/polyaniline hydrogel heterostructures. *ACS Nano* **7**, 3540–3546 (2013).
64. Lin, Y. et al. Porous enzymatic membrane for nanotextured glucose sweat sensors with high stability toward reliable noninvasive health monitoring. *Adv. Funct. Mater.* **29**, 1902521 (2019).
65. Vaddiraju, S. et al. Design and fabrication of a high-performance electrochemical glucose sensor. *J Diabetes Sci. Technol.* **5**, 1044–1051 (2011).
66. Yang, W., Zhou, H. & Sun, C. Synthesis of ferrocene-branched chitosan derivatives: redox polysaccharides and their application to reagentless enzyme-based biosensors. *Macromol. Rapid Commun.* **28**, 265–270 (2007).
67. Pietschnig, R. Polymers with pendant ferrocenes. *Chem Soc Rev* **45**, 5216–5231 (2016).
68. Mao, F., Mano, N. & Heller, A. Long tethers binding redox centers to polymer backbones enhance electron transport in enzyme "Wiring" hydrogels. *J. Am. Chem. Soc.* **125**, 4951–4957 (2003).
69. Yang, Y. et al. A laser-engraved wearable sensor for sensitive detection of uric acid and tyrosine in sweat. *Nat. Biotechnol.* **38**, 217–224 (2020).
70. Li, J. et al. A tissue-like neurotransmitter sensor for the brain and gut. *Nature* **606**, 94–101 (2022).
71. Scholz, F. Voltammetric techniques of analysis: the essentials. *ChemTexts* **1**, 17 (2015).
72. Rahman, M. M. & Lee, J.-J. Electrochemical dopamine sensors based on graphene. *J. Electrochem. Sci. Technol.* **10**, 185–195 (2019).
73. Jiang, J. & Du, X. Sensitive electrochemical sensors for simultaneous determination of ascorbic acid, dopamine, and uric acid based on Au@Pd-reduced graphene oxide nanocomposites. *Nanoscale* **6**, 11303–11309 (2014).
74. Wang, Z. et al. Simultaneous and selective measurement of dopamine and uric acid using glassy carbon electrodes modified with a complex of gold nanoparticles and multiwall carbon nanotubes. *Sens. Actuat. B: Chem.* **255**, 2069–2077 (2018).
75. Zhang, C., Losego, M. D. & Braun, P. V. Hydrogel-based glucose sensors: effects of phenylboronic acid chemical structure on response. *Chem. Mater.* **25**, 3239–3250 (2013).
76. Csoeregi, E., Schmidtke, D. W. & Heller, A. Design and optimization of a selective subcutaneously implantable glucose electrode based on "Wired" glucose oxidase. *Anal. Chem.* **67**, 1240–1244 (1995).
77. Han, X. X., Rodriguez, R. S., Haynes, C. L., Ozaki, Y. & Zhao, B. Surface-enhanced Raman spectroscopy. *Nat. Rev. Methods Primers* **1**, 87 (2021).
78. Tang, W. et al. Touch-based stressless cortisol sensing. *Adv. Mater.* **33**, 2008465 (2021).
79. Nezhadali, A. & Khalili, Z. Computer-aided study and multivariate optimization of nanomolar metformin hydrochloride analysis using molecularly imprinted polymer electrochemical sensor based on silver nanoparticles. *J. Mater. Sci.: Mater. Electron.* **32**, 27171–27183 (2021).
80. Wang, B. et al. Wearable aptamer-field-effect transistor sensing system for noninvasive cortisol monitoring. *Sci. Adv.* **8**, eabk0967 (2022).
81. Lee, Y. et al. Wireless, intraoral hybrid electronics for real-time quantification of sodium intake toward hypertension management. *Proc. Natl Acad. Sci. USA* **115**, 5377–5382 (2018).
82. Shirzaei Sani, E. et al. A stretchable wireless wearable bioelectronic system for multiplexed monitoring and combination treatment of infected chronic wounds. *Sci. Adv.* **9**, eadf7388 (2023).
83. Nyein, H. Y. Y. et al. A wearable electrochemical platform for noninvasive simultaneous monitoring of Ca2+ and pH. *Acs Nano* **10**, 7216–7224 (2016).

84. Zea, M. et al. Enhanced performance stability of iridium oxide-based pH sensors fabricated on rough inkjet-printed platinum. *ACS Appl. Mater. Interfaces* **11**, 15160–15169 (2019).
85. Yang, Y. & Gao, W. Wearable pH sensing beyond the Nernst limit. *Nat. Electron.* **1**, 580–581 (2018).
86. Hosseini, S., Vázquez-Villegas, P., Rito-Palomares, M. & Martinez-Chapa, S. O. in *Enzyme-linked Immunosorbent Assay (ELISA): From A to Z* (eds Hosseini, S., Vázquez-Villegas, P., Rito-Palomares, M., & Martinez-Chapa, S. O.) 67–115 (Springer Singapore, 2018).
87. Surugiu, I., Danielsson, B., Ye, L., Mosbach, K. & Haupt, K. Chemiluminescence imaging ELISA using an imprinted polymer as the recognition element instead of an antibody. *Anal. Chem.* **73**, 487–491 (2001).
88. Breault-Turcot, J., Poirier-Richard, H.-P., Couture, M., Pelechacz, D. & Masson, J.-F. Single chip SPR and fluorescent ELISA assay of prostate specific antigen. *Lab Chip* **15**, 4433–4440 (2015).
89. de la Rica, R. & Stevens, M. M. Plasmonic ELISA for the detection of analytes at ultralow concentrations with the naked eye. *Nat. Protoc.* **8**, 1759–1764 (2013).
90. Gao, Y. et al. A flexible multiplexed immunosensor for point-of-care in situ wound monitoring. *Sci. Adv.* **7**, eabg9614 (2021).
91. Dervisevic, M. et al. Transdermal electrochemical monitoring of glucose via high-density silicon microneedle array patch. *Adv. Funct. Mater.* **32**, 2009850 (2022).
92. He, R. et al. A colorimetric dermal tattoo biosensor fabricated by microneedle patch for multiplexed detection of health-related biomarkers. *Adv. Sci.* **8**, 2103030 (2021).
93. Han, J. H. et al. Microneedles coated with composites of phenylboronic acid-containing polymer and carbon nanotubes for glucose measurements in interstitial fluids. *Biosens. Bioelectron.* **238**, 115571 (2023).
94. Zhang, P. et al. Wearable transdermal colorimetric microneedle patch for Uric acid monitoring based on peroxidase-like polypyrrole nanoparticles. *Anal. Chim. Acta* **1212**, 339911 (2022).
95. Pu, Z. et al. A thermal activated and differential self-calibrated flexible epidermal biomicrofluidic device for wearable accurate blood glucose monitoring. *Sci. Adv.* **7**, eabd0199 (2021).
96. Chen, Y. et al. Skin-like biosensor system via electrochemical channels for noninvasive blood glucose monitoring. *Sci. Adv.* **3**, e1701629 (2017).
97. Rock, K. L., Kataoka, H. & Lai, J.-J. Uric acid as a danger signal in gout and its comorbidities. *Nat. Rev. Rheumatol.* **9**, 13–23 (2013).
98. Laffel, L. Ketone bodies: a review of physiology, pathophysiology and application of monitoring to diabetes. *Diabetes/metabolism Res. Rev.* **15**, 412–426 (1999).
99. Blau, N., Van Spronsen, F. J. & Levy, H. L. Phenylketonuria. *Lancet* **376**, 1417–1427 (2010).
100. Teymourian, H. et al. Microneedle-based detection of ketone bodies along with glucose and lactate: toward real-time continuous interstitial fluid monitoring of diabetic ketosis and ketoacidosis. *Anal. Chem.* **92**, 2291–2300 (2020).
101. Derbyshire, P. J., Barr, H., Davis, F. & Higson, S. P. J. Lactate in human sweat: a critical review of research to the present day. *J. Physiol. Sci.* **62**, 429–440 (2012).
102. Bollella, P., Sharma, S., Cass, A. E. G. & Antiochia, R. Microneedle-based biosensor for minimally-invasive lactate detection. *Biosens. Bioelectron.* **123**, 152–159 (2019).
103. Caliò, A. et al. Polymeric microneedles based enzymatic electrodes for electrochemical biosensing of glucose and lactic acid. *Sens. Actuat. B: Chem.* **236**, 343–349 (2016).
104. De la Paz, E. et al. Non-invasive monitoring of interstitial fluid lactate through an epidermal iontophoretic device. *Talanta* **254**, 124122 (2023).
105. Sempionatto, J. R. et al. Epidermal enzymatic biosensors for sweat vitamin C: toward personalized nutrition. *ACS Sensors* **5**, 1804–1813 (2020).
106. Zhao, J. et al. A wearable nutrition tracker. *Adv. Mater.* **33**, 2006444 (2021).
107. Tai, L.-C. et al. Methylxanthine drug monitoring with wearable sweat sensors. *Adv Mater* **30**, 1707442 (2018).
108. Li, H. et al. Microneedle-based potentiometric sensing system for continuous monitoring of multiple electrolytes in skin interstitial fluids. *ACS Sensors* **6**, 2181–2190 (2021).
109. Zhu, D. D. et al. Microneedle-coupled epidermal sensors for in-situ-multiplexed ion detection in interstitial fluids. *ACS Appl. Mater. Interf.* **15**, 14146–14154 (2023).
110. Molinero-Fernández, Á., Casanova, A., Wang, Q., Cuartero, M. & Crespo, G. A. In vivo transdermal multi-ion monitoring with a potentiometric microneedle-based sensor patch. *ACS Sensors* **8**, 158–166 (2023).
111. Lee, W. et al. Conformable microneedle pH sensors via the integration of two different siloxane polymers for mapping peripheral artery disease. *Sci. Adv.* **7**, eabi6290 (2021).
112. Dervisevic, M. et al. Wearable microneedle array-based sensor for transdermal monitoring of pH levels in interstitial fluid. *Biosens. Bioelectron.* **222**, 114955 (2023).
113. Ghoneim, M. T. et al. Recent progress in electrochemical pH-sensing materials and configurations for biomedical applications. *Chem. Rev.* **119**, 5248–5297 (2019).
114. Kiang, T. K., Schmitt, V., Ensom, M. H., Chua, B. & Häfeli, U. O. Therapeutic drug monitoring in interstitial fluid: a feasibility study using a comprehensive panel of drugs. *J. Pharm. Sci.* **101**, 4642–4652 (2012).
115. Bhake, R. et al. Continuous free cortisol profiles in healthy men: validation of microdialysis method. *J. Clin. Endocrinol. Metab.* **105**, e1749–e1761 (2020).
116. Venugopal, M., Arya, S. K., Chornokur, G. & Bhansali, S. A realtime and continuous assessment of cortisol in ISF using electrochemical impedance spectroscopy. *Sens. Actuat. A: Phys.* **172**, 154–160 (2011).
117. Ryabkova, V. A., Churilov, L. P. & Shoenfeld, Y. Influenza infection, SARS, MERS and COVID-19: cytokine storm–the common denominator and the lessons to be learned. *Clin. Immunol.* **223**, 108652 (2021).
118. Xu, J., Yang, B., Kong, J., Zhang, Y. & Fang, X. Real-time monitoring and early warning of a cytokine storm in vivo using a wearable noninvasive skin microneedle patch. *Adv. Healthcare Mater.* **12**, 2203133 (2023).
119. Zhang, X., Chen, G., Bian, F., Cai, L. & Zhao, Y. Encoded microneedle arrays for detection of skin interstitial fluid biomarkers. *Adv. Mater.* **31**, 1902825 (2019).
120. Bao, L., Park, J., Qin, B. & Kim, B. Anti-SARS-CoV-2 IgM/IgG antibodies detection using a patch sensor containing porous microneedles and a paper-based immunoassay. *Sci. Rep.* **12**, 10693 (2022).
121. Wang, Z. et al. Microneedle patch for the ultrasensitive quantification of protein biomarkers in interstitial fluid. *Nat. Biomed. Eng.* **5**, 64–76 (2021).
122. Teymourian, H. et al. Wearable electrochemical sensors for the monitoring and screening of drugs. *ACS sensors* **5**, 2679–2700 (2020).
123. Zeitlinger, M. A. et al. Protein binding: do we ever learn? *Antimicrob. Agents Chemother.* **55**, 3067–3074 (2011).
124. Rawson, T. M. et al. Microneedle biosensors for real-time, minimally invasive drug monitoring of phenoxymethylpenicillin: a first-in-human evaluation in healthy volunteers. *Lancet Digital Health* **1**, e335–e343 (2019).
125. Zhang, X. et al. Photoinduced regeneration of an aptamer-based electrochemical sensor for sensitively detecting adenosine triphosphate. *Anal. Chem.* **90**, 4968–4971 (2018).
126. Nichols, S. P., Koh, A., Storm, W. L., Shin, J. H. & Schoenfisch, M. H. Biocompatible materials for continuous glucose monitoring devices. *Chem. Rev.* **113**, 2528–2549 (2013).

127. Xie, X. et al. Reduction of measurement noise in a continuous glucose monitor by coating the sensor with a zwitterionic polymer. *Nat. Biomed. Eng.* **2**, 894–906 (2018).
128. Kim, D. W., Kong, M. & Jeong, U. Interface design for stretchable electronic devices. *Adv. Sci.* **8**, 2004170 (2021).
129. Zhao, Y. et al. Soft strain-insensitive bioelectronics featuring brittle materials. *Science* **378**, 1222–1227 (2022).
130. Sinha, M. et al. A comparison of time delay in three continuous glucose monitors for adolescents and adults. *J. Diabetes Sci. Technol.* **11**, 1132–1137 (2017).
131. Facchinetti, A., Sparacino, G. & Cobelli, C. Reconstruction of glucose in plasma from interstitial fluid continuous glucose monitoring data: role of sensor calibration. *J. Diabetes Sci. Technol.* **1**, 617–623 (2007).
132. Bequette, B. W. Continuous glucose monitoring: real-time algorithms for calibration, filtering, and alarms. *J. Diabetes Sci. Technol.* **4**, 404–418 (2010).
133. Makvandi, P. et al. Engineering microneedle patches for improved penetration: analysis, skin models and factors affecting needle insertion. *Nano-Micro Lett.* **13**, 1–41 (2021).
134. Wang, S. et al. Electrochemical impedance spectroscopy. *Nat. Rev. Methods Primers* **1**, 41 (2021).
135. Parrilla, M. et al. Wearable all-solid-state potentiometric microneedle patch for intradermal potassium detection. *Anal. Chem.* **91**, 1578–1586 (2018).
136. Xu, C., Yang, Y. & Gao, W. Skin-interfaced sensors in digital medicine: from materials to applications. *Matter* **2**, 1414–1445 (2020).
137. Song, S., Zhang, H., Wan, Y. & Luo, J. 3D neighborhood nanostructure reinforces biosensing membrane. *Adv. Funct. Mater.* **33**, 2303313 (2023).
138. Lee, H. et al. A graphene-based electrochemical device with thermoresponsive microneedles for diabetes monitoring and therapy. *Nat. Nanotechnol.* **11**, 566–572 (2016).
139. Parlak, O., Keene, S. T., Marais, A., Curto, V. F. & Salleo, A. Molecularly selective nanoporous membrane-based wearable organic electrochemical device for noninvasive cortisol sensing. *Sci. Adv.* **4**, eaar2904 (2018).
140. Tang, L., Chang, S. J., Chen, C.-J. & Liu, J.-T. Non-invasive blood glucose monitoring technology: a review. *Sensors* **20**, 6925 (2020).
141. Hersini, K. J., Melgaard, L., Gazerani, P. & Petersen, L. J. Microdialysis of inflammatory mediators in the skin: a review. *Acta dermato-venereologica* **94**, 501–511 (2014).

Acknowledgements

This work was supported by the National University of Singapore (NUS) Institute for Health Innovation and Technology (iHealthtech) Seed Grant (A-0001415-06-00), the NUS Start-Up Grant (A-0009363-03-00), and the NUSS Professorship Grant (E-468-00-0012-01).

Author contributions

Z.X.W. and Z.Q. made equal contributions to writing and revising all sections. S.W.C. authored certain sections, enhancing all figures, texts, and overall organization. C.T.L. led the project, formulated the content plan, and revised all sections. S.C.F., Y.C.L. and J.M.Q. contributed to writing the first draft. All authors contributed to reviewing and enhancing the manuscript.

Competing interests

The authors declare no competing interests.

Additional information

Supplementary information The online version contains supplementary material available at https://doi.org/10.1038/s43246-024-00468-6.

Correspondence and requests for materials should be addressed to Shuwen Chen or Chwee Teck Lim.

Peer review information *Communications Materials* thanks Minqiang Wang and the other, anonymous, reviewer(s) for their contribution to the peer review of this work. Primary Handling Editor: John Plummer. A peer review file is available.

Reprints and permissions information is available at http://www.nature.com/reprints

Publisher's note Springer Nature remains neutral with regard to jurisdictional claims in published maps and institutional affiliations.

Open Access This article is licensed under a Creative Commons Attribution 4.0 International License, which permits use, sharing, adaptation, distribution and reproduction in any medium or format, as long as you give appropriate credit to the original author(s) and the source, provide a link to the Creative Commons licence, and indicate if changes were made. The images or other third party material in this article are included in the article's Creative Commons licence, unless indicated otherwise in a credit line to the material. If material is not included in the article's Creative Commons licence and your intended use is not permitted by statutory regulation or exceeds the permitted use, you will need to obtain permission directly from the copyright holder. To view a copy of this licence, visit http://creativecommons.org/licenses/by/4.0/.

© The Author(s) 2024